ChemComm

Accepted Manuscript

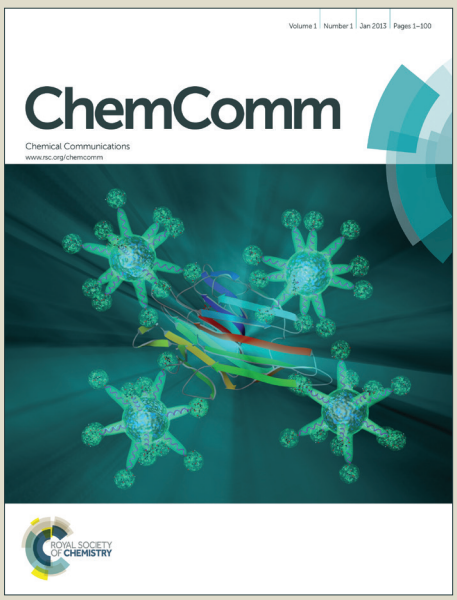

ROYAL SOCIETY OF CHEMISTRY

www.rsc.org/chemcomm

Journal Name

COMMUNICATION

One-step Carbonization Route to Nitrogen-doped Porous Carbon Hollow Spheres with Ultrahigh Nitrogen Content for CO_2 Adsorption

Received 00th January 20xx,
Accepted 00th January 20xx

DOI: 10.1039/x0xx00000x

www.rsc.org/

Yu Wang,[a] Houbing Zou,[a] Shangjing Zeng,[a] Ying Pan,[a] Runwei Wang,*[a] Xue Wang,[a] Qingli Sun,[a] Zongtao Zhang,[a] and Shilun Qiu[a]

Nitrogen doped porous carbon hollow spheres (N-PCHS) with ultrahigh nitrogen content of 15.9 wt% and high surface area of 775 $m^2 \cdot g^{-1}$ were prepared using Melamine-Formaldehyde nanospheres as hard templates and nitrogen source. The N-PCHS were completely characterized and were found to exhibit considerable CO_2 adsorption performance(4.42 $mmol \cdot g^{-1}$).

Porous carbon hollow nanostructures have attracted increasing attention because of their unique properties such as low density, high surface-to-volume ratio, shell permeability, good chemical stability and electrical conductivity. They have also exhibited promising applications in catalysis,[1, 2] adsorption,[3-5] lithium-ion batteries[6, 7] and oxygen reduction reactions.[8] At the same time, the intrinsic chemical inertness of carbon materials also limits their performance in the above-mentioned applications, in this regard, previous reports suggested that modification of carbon matrix with heteroatoms (N, S and P) [5,9-11] can minimize such limitations. Among several possible choices, nitrogen doping has been studied widely, and relevant researches revealed that the surface polarity, electrical conductivity, surface basic sites and electron-donor tendency can be improved largely through such doping.[12-16]

Generally, there are two approaches available for successfully introducing nitrogen into porous carbon matrix, which can be broadly categorized into using N-containing gas (NH_3)[17] and using N-rich solid reagents[9 ,18] as N source. Comparing with N-containing gas (NH_3), N-rich solid reagents such as melamine (67 wt% N) and urea (47 wt% N) possess strong interaction with carbon matrix, which can efficiently introduce N into carbon matrix via hydrothermal treatment or carbonization. However, there have been only a few papers to-date on the synthesis and application of N-doped porous carbon hollow nanostructures. Oh's group reported preparation of N-doped hollow carbon spheres through pyrolysis of core–shell ZIF-8@polystyrene spheres.[4] Han etal used sulfonated polystyrene spheres as templates and polyaniline as N source for fabricating N-doped hollow carbon spheres with a high nitrogen content of 6.7 %.[19] Recently, Zhao's group also reported synthesis of N-doped hollow carbon spheres exhibiting considerable performance in CO_2 capture using SiO_2 spheres as hard templates and melamine as N source.[5] Although the obtained materials exhibited high nitrogen content and high surface area, these strategies involved removal of the hard templates, which is multistep, complex, time-consuming, and requires hazardous reagents (HF solution). Moreover, KOH or CO_2 are used in some activation processes to obtain materials with high porosity.[9,20,21] Therefore, it still remains a great challenge to prepare N-doped porous carbon hollow nanostructures with high nitrogen content and high surface area through a simple and efficient process.

Herein, we report a one-step carbonization route to Nitrogen-doped Porous Carbon Hollow Spheres (N-PCHS) using melamine-formaldehyde (MF) nanospheres both as a hard template and the nitrogen source and resorcinol-formaldehyde (RF) resin as carbon precursor. The core-shell MF@RF spheres were first prepared through coating the MF nanospheres with a uniform RF shell via sol-gel process. When carbonizing the MF@RF spheres under Ar atmosphere, the internal MF core transformed to N-rich gas and the external RF shell transformed to porous carbon framework, which is attributed to the difference in their frameworks. Importantly, with slowly effused of the N-rich gas from interior, nitrogen atom was effectively introduced into the outer carbon matrix, resulting in N-PCHS. Owing to the activation process of the other acidic gases, the obtained N-PCHS showed abundant pores, high surface area (775 $m^2 \cdot g^{-1}$) and ultrahigh nitrogen content (8.9 wt% even under a carbonization at 900). Furthermore, the N-PCHS exhibited considerable CO_2 sorption performance with a capacity of 4.42 $mmol \cdot g^{-1}$, a notable value among porous carbon materials.

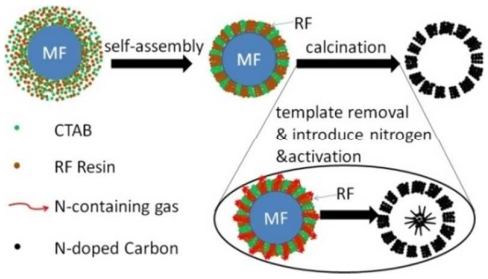

[a] College of Chemistry and State Key Laboratory of Inorganic Synthesis and Preparative Chemistry, Jilin University, Changchun 130012, China. E-mail: rwwang@jlu.edu.cn.

Electronic Supplementary Information (ESI) available: [details of any supplementary information available should be included here]. See

Scheme 1 Illustration of the formation process of the N-PCHS.

The fabrication process of N-PCHS is illustrated in Scheme 1. First, MF nanospheres with a diameter of approximately 300 nm (Fig.S1A) were synthesized via a hydrothermal process. Then the MF nanospheres were coated with uniform RF shells via a sol-gel process, [2] leading to the formation of core-shell MF@RF spheres. The SEM and TEM image in Fig.S2 revealed that the MF@RF possessed a spherical morphology with a diameter of approximately 500 nm, suggesting a RF shell with a thickness of 100 nm. Finally, the N-PCHS was obtained after a simple carbonization process. From the TEM image (shown in Fig.1B), a hollow sphere with a shell thickness of 50 nm could be clearly observed. Additionally, some broken spheres indicated by white arrows also provided evidence of a hollow structure (Fig.1A). As typically observed in the synthesis of porous carbon materials, the RF shell and the MF@RF spheres in the current work also experienced shrinkage during calcination, and the thickness of RF shell and the diameter reduced to 50 nm and 300 nm, respectively. Furthermore, to understand the formation process of the hollow structure, we also carbonized the MF@RF spheres at lower temperature from 600 ℃ to 800 ℃. Interestingly, the core-shell structure first transformed to a yolk-shell structure, as shown in the TEM images of Fig.1, and then to hollow carbon sphere. It is worth mentioning that no residue was observed in the void space in the hollow interior of the sample obtained at 800 ℃ from TEM image, which was consistent with the TG result (Fig. S2) that only 2.38 wt% residue was present for MF after 800 ℃ carbonization. These results clearly revealed that the internal MF core gradually decomposed to some gases effusing out while the external RF shell transformed to porous carbon framework, along with the pyrolysis of core-shell structured MF@RF spheres. [18, 22]

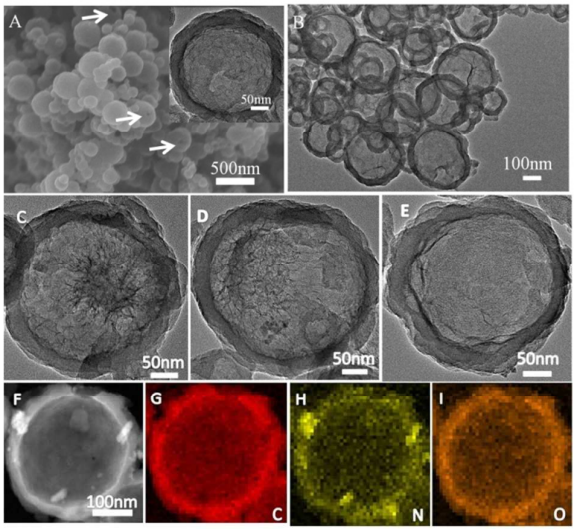

Fig. 1 (A) SEM and (B) TEM image of N-PCHS obtained via carbonizing at 900 ℃, and the inset in (A) is the TEM image of single N-PCHS. TEM images of sample obtained via carbonizing at different temperature (C) 600 ℃, (D) 700℃, (E) 800℃. (F) STEM image and the corresponding elemental mapping of (G) C, (H) N, (I) O of single N-PCHS.

The structure and framework of N-PCHS carbonized at 900 ℃ were further investigated by the STEM and X-ray photoelectron spectroscopy (XPS) analyses. The STEM image of single N-PCHS sphere, as shown in Fig. 1F, further confirms the hollow nanostructure with a shell thickness of about 50 nm. The corresponding elemental mapping (Fig.1G, H, I) also showed a homogeneous distribution of C, N and O elements. Moreover, XPS spectra were obtained to get more information about the surface states of N-PCHS, showing three typical peaks of C1s, N1s and O1s (Fig.S4), and the corresponding content of every elements are also displayed. The spectrum of N1s can be resolved into three peaks (Fig.S5), pyridinc-N (398.3 eV, 30.87%), pyrrolic-/pyridonic-N (400 eV, 2.75%) and graphitic-type quaternary-N structure (401 eV, 66.38%),[9, 23-25] which correspond to disordered graphitic structure derived from the XRD spectra.[22] In addition, the peak at 287.71 eV resolved from the spectrum of C1s (Fig.S6) suggests the existence of C=N bond[26]. It is well known that graphitic-type quaternary-N is the most stable functionality at temperatures higher than 600 ℃. [27] This can explain the increase in proportion of the graphitic-type quaternary-N with respect to the total nitrogen content, as observed from the XPS spectra, when the carbonization temperature was raised. The relative IR spectra (Fig.S3) show bands at 1248 cm^{-1} and 1589 cm^{-1}, which can be assigned to the vibrations of aromatic C–N stretching bond and aromatic ring, respectively.[28] The weak band at 1390 cm^{-1} suggests the presence of the C-N stretching vibration and the existence of triazine rings in the carbon matrix.[9] Furthermore, the elemental analysis results revealed that the N-PCHS-900 is composed of C, H, N, and O elements, and the nitrogen content was as high as 8.9 wt% (Table S1), which was corresponds well with the EDX results (Fig. S8). The nitrogen content of N-PCHS obtained through carbonizing at 600 ℃was as high as 15.9 wt%. All these results clearly indicated that nitrogen was effectively doped into the framework of hollow C shell and the hard template MF sphere could be effectively removed via this one-step carbonization route.

The pore structure and BET surface area of N-PCHS-900 were also studied by nitrogen sorption analysis. The nitrogen sorption isotherm shows a type IV curve with a H4 hysteresis loop and a distinct uptake condensation step in the range of $P/P_0 < 0.1$. The distinct uptake at low pressure indicates the existence of abundant micropore structure. The hysteresis loop at $0.45 < P/P_0 < 0.9$ can be attributed to the large void space (hollow interior) of the N-PCHS-900. Moreover, a sudden drop in P/P_0 at about 0.5 in the desorption branch could also be observed, which is in agreement with the phenomenon of a large pore encapsulated by a matrix with relatively small pore sizes. Owing to this hierarchical porous structure, the N-PCHS-900 exhibited a high BET surface area of 775 $m^2.g^{-1}$, of which the micropore surface area was 630 $m^2.g^{-1}$.

A point to note is that the nitrogen content of N-PCHS-900 measured via XPS analysis (2.02 wt%) was far less than that obtained from the elemental analysis (8.9 wt%). This result suggested that the nitrogen content of the inner surface of the hollow C shell was higher than that of the outer surface, considering the fact that XPS is a surface analysis technique (5 nm thickness). The above observation can be explained as follows. The gas stream was dissolved in deionized water during carbonization under Ar atmosphere. As expected, the pH value of the collected solution was about 9, indicating the formation of some N-rich alkaline gases such as NH_3 [29,30] from the internal MF core during the carbonization process. Prior research has reported that N-rich alkaline gases are the direct nitrogen source to introduce nitrogen

atoms into carbon framework.[17] Since N-rich gases , continuously produced in situ, gradually effused out from hollow interior and flowed through the RF shell, it is reasonable to argue that the nitrogen content of the inner surface of the hollow C shell was higher than that of the outer surface after completion of the carbonization. Along with these N-rich alkaline gases, some acidic gases, such as CO_2 were also produced, which reacted with the carbon shell (CO_2+C=CO) to activate the carbon shell to generate more micropores. [22] This was also demonstrated by the nitrogen sorption analysis, in which both the uptake amount at low pressure (P/P_0 < 0.1) and the micropore surface area of relevant samples increased with the rised carbonization temperature (Table S2). To summarize, this one-step carbonization method involves three different processes at the same time: removal of template, introduction of nitrogen and activation of the C shell. Compared with other hard template approaches (such as SiO_2 spheres), obviously, this strategy exhibits several advantages: (1) it is facial and simple through a one-step route; (2) the N atom can be doped into the framework more efficiently; (3) the activation of gases endows the hollow shell more abundant pore structures.

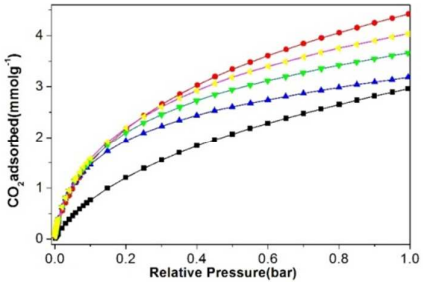

Fig. 2 CO_2 adsorption isotherms at 273K of N-PCHS obtained at different carbonization temperature: 900 ℃ (red), 800℃(yellow), 700 ℃ (green), 600 ℃ (blue); CO_2 adsorption isotherm at 298K of N-PCHS-900 (black).

Since our N-PCHS-900 possessed fine micropore area (630 $m^2 \cdot g^{-1}$) and high nitrogen content (8.39 wt%), the potential of our N-PCHSs in CO_2 adsorption were further examined. The relevant sorption isotherms for N-PCHS-900 show an adsorption of CO_2 of 4.42 $mmol \cdot g^{-1}$ at 1.0 bar and 273K and even 2.96 $mmol \cdot g^{-1}$ at 298K, which are higher than many other materials[5], and even match with some activated carbon samples[9,31], as illustrate in table S3. CO_2 uptake at 273K and 1.0 bar for N-PCHSs prepared at the temperature of 600, 700, 800 were also performed and showed capacities of 3.19, 3.66, and 4.04 $mmol \cdot g^{-1}$, respectively, whereas the nitrogen content decreases steadily in the same order(Table S2). As well known, the key factors contribute to the CO_2 uptake at ambient conditions are ultramicropores (micropores ≤ 0.7nm) [32,33] and presence of basic sites, like suitable nitrogen species [20,23, 32,33]. According to previous reports, nitrogen species facilitate CO_2 uptake through forming N–H···O hydrogen bond [34]. Considering that our H-PCHSs contain mainly pyridine and quaternary-N structure, which can not form hydrogen bonds with CO_2 molecules, we believe that ultramicropore is the leading factor in CO_2 uptake for our N-PCHSs. As expected, the total surface area, micropore surface area and ultramicropore volume of our samples increased significantly with elevated carbonization temperature (Table. S2). The increment in surface area to N ratio (from 22.94 to 92.37, Table S2) further confirms our hypothesis. This is also in line with Sethia's result that CO_2 uptake is strongly dependent on the occurrence of ultramicropores and much less on the nitrogen content [35]. N_2 adsorption at 273 K and 298 K were also performed as comparisons (Figure S11, S12). Based on the initial slopes of N_2 and CO_2 adsorption isotherms, the adsorption selectivity for CO_2 to N_2 of the sample N-PCHS-900 was 35 at 273K and 21 at 298 K, respectively. The selectivity was also higher than many other carbon materials (table S4). Since our strategy is facial and simple, it can offer more opportunity for future practical application in CO_2 adsorption.

In summary, we have developed a novel and feasible one-step carbonization strategy to prepare nitrogen-doped porous carbon hollow spheres using MF spheres as both hard template and nitrogen source and RF resin as carbon precursor. While the external RF shell transformed to porous carbon framework, the MF sphere gradually decomposed to some gases effusing out. The N rich alkaline gases can efficiently introduce nitrogen into the C shell. Moreover, the acidic gases such as CO_2 can activate the C shell to produce more micropores. As a result, the obtained N-PCHS exhibited a high nitrogen loading content (8.9 wt% even under a carbonization at 900℃) and high surface area of 775 $m^2 \cdot g^{-1}$. Owing to the hollow nanostructure, abundant micropores and ultrahigh nitrogen doping content, the resultant N-PCHS showed considerable performance in CO_2 capture with a capacity of 4.42 $mmol \cdot g^{-1}$ and good selectivity. Considering the unique feature of our samples (hierarchical pore hollow structure, nitrogen doped with some degree of graphitization) and the flexibility of this strategy, we believe that this efficient strategy would offer a platform for designing multifunctional yolk-shell metal/bimetal@N-PCHS and even N-doped metal-oxide hollow structure for applications, such as adsorbents and energy storage, relevant research is currently being investigated.

This work was supported by National Natural Science Foundation of China (21390394), the National Basic Research Program of China (2012CB821700, 2011CB808703), NSFC (21261130584, 91022030), "111" project (B07016), Award Project of KAUST (CRG-1-2012-LAI-009) and Ministry of Education, Science and Technology Development Center Project (20120061130012).

Notes and references

[1] X. Fang, J. Zang, X. Wang, M. Zheng, N. Zheng, *J. Mater. Chem. A.* 2014, **2**, 6191.
[2] B. Guan, X. Wang, Y. Xiao, Y. Liu, Q. Huo, *Nanoscale.*, 2013, **5**, 2469.
[3] B. Chang, W. Shi, D. Guan, Y. Wang, B. Zhou, X. Dong, *Materials Letter.,* 2014, **126**, 13.; K. S. Lakhi, W. S. Cha , S. Joseph, B. J. Wood, S. S. Aldeyab, G. Lawrence, J. H. Choy, A. Vinu, *Catalysis Today*, 2015 , **243**, 209.
[4] H. J. Lee, S. Choi, M. Oh, *Chem. Commun.*, 2014, **50**, 4492; K. S. Lakhi, A. V. Baskar, J. S. M. Zaidi, S. S. A. Deyab, M. El-Newehy, J. H Choy, A. Vinu, *RSC Adv.*, 2015, **5**, 40183.
[5] S. Feng, W. Li, Q. Shi, Y. Li, J. Chen, Y. Ling, A. M. Asiri, D. Zhao, *Chem. Commun.*, 2014, **50**, 329.
[6] H. Gao, C. Liu, Y. Liu, Z. Liu, W. Dong, *Materials Chemistry and Physics.*, 2014, **147**, 218; J. Zhu, K. Sakaushi, G. Clavel, M. Shalom , M. Antonietti , T. P. Fellinger, *J. Am. Chem. Soc.*, 2015, **137**, 5480.
[7] G. Zhang, L. Yu, H. Wu, H. E. Hoster ,X. Lou, *Advanced Materials.*,2012, **24**, 4609; M. Ledendecker, G. Clavel, M. Antonietti, M. Shalom, *Adv. Funct. Mater,* 2015, **25**, 393.
[8] C. Hsu, J. Jan, H. Lin , P. Kuo, *New J. Chem.*, 2014,**38**, 5521.

[9] J. Yu, M. Guo, F. Muhammad, A. Wang, F. Zhang, Q. Li, G. Zhu, *Carbon.*, 2014, **69**, 502.
[10] W. Zhou, X. Xiao, M. Cai, L. Yang, *Nano Lett.*,2014, **14**, 5250.
[11] Y. Zhang, T. Mori, J. Ye, M. Antonietti, *J. Am. Chem. Soc.*, 2010, **132**, 6294.
[12] T. Schiros, D. Nordlund, L. Palova´, D. Prezzi, L. Zhao, K. S. Kim, U. Wurstbauer, C. Gutierrez´, D. Delongchamp, C. Jaye, D. Fischer, H. Ogasawara, L. G. M. Pettersson, D. R. Reichman, P. Kim, M. S. Hybertsen, A. N. Pasupathy, *Nano Lett.*, 2012, **12** , 4025.
[13] R. Czerw, M. Terrones, J. C. Charlier, X. Blase, B. Foley, R. Kamalakaran, N. Grobert, H. Terrones, D. Tekleab, P. M. Ajayan, W. Blau, M. Rühle, D. L. Carroll, *Nano Letters.*, 2001, **1**, 457.
[14] Z. Ding, L. Zhao, L. Suo, Y. Jiao, S. Meng, Y. S. Hu, Z. Wang, L. Chen, Phys. *Chem. Chem. Phys.*, 2011, **13**, 15127.
[15] Y. F. Li, Z. Zhou, L. B. Wang, *J. Chem. Phys.*, 2008, **129**, 104703.
[16] K. N. Wood, R. O'Hayre, S. Pylypenko, *Energy Environ. Sci.*, 2014,**7**, 1212.
[17] J. Liu, S. Webster, D. L. Carroll, *J. Phys. Chem. B.*, 2005, **109**, 15769.
[18] Z. Wu, P. A. Webley, D. Zhao, *J. Mater. Chem.*, 2012, **22**, 11379.
[19] J. Han, G. Xu, B. Ding, J. Pan, H. Dou, D. R. MacFarlane, *J. Mater. Chem. A.*, 2014, **2**, 5352.
[20] N. P. Wickramaratne, M. Jaroniec, ACS Appl. *Mater. Interfaces.*, 2013, **5**, 1849.
[21] T. Yang, J. Liu, R. Zhou, Z. Chen, H. Xu, S. Z. Qiao, M. J. Monteiro, *J. Mater. Chem. A.*, 2014, **2**, 18139.
[22] M. Sevilla, A. B. Fuertes, *ACS Nano.*, 2014, **8**, 5069; K. K. R. Datta, V. V. Balasubramanian, K. Ariga, T. Mori, A. Vinu. *Chem. Eur. J.*, 2011, **17**, 3390.
[23] N. P. Wickramaratne, J. Xu, M.Wang, L. Zhu, L. Dai, M. Jaroniec, *Chem. Mater.*, 2014, 26, 2820.
[24] A. D. Marczewska, J. Goworek, S. Pikus, E. Kobylas, *Langmuir.*, 2002, **18**, 7538.
[25] X. Jin, V. V. Balasubramanian, S. T. Selvan, D. P. Sawant, M. A. Chari, G. Q. Lu, A. Vinu, *Angew. Chem.*, 2009, **121**, 8024.
[26] D. Feng, Z. Zhou, M. Bo, *Polymer Degradation and Stability.*, 1995,**50**,65.
[27] A. N. Márqueza, I. Esparteroa, J. C. Lazob, A. Romeroa, J. L. Valverde, *Chemical Engineering Journal.*, 2009, **153**, 211.
[28] A. Chen, Y. Yu, H. Lv, Y. Wang, S. Shen, Y. Hu, B. Li, Y. Zhang, J. Zhang, *J. Mater. Chem. A.*, 2013, **1**, 1045.
[29] B. Friedel, S. G. Weber, *small.*, 2006, **2**, 859.
[30] H. Zhong, H. Zhang, S. Liu, C. Deng, M. Wang, *ChemSusChem.*, 2013, **6**, 807.
[31] A. Chen, Y. Yua, Y. Zhang, W. Zang, Y. Yu, Y. Zhang, S. Shen, J. Zhang, *Carbon.*, 2014, **80**, 19.
[32] L. Wang, R. T. Yang, *J. Phys. Chem. C.*, 2012, **116**, 1099.
[33] N. P. Wickramaratne, M. Jaroniec, *J. Mater. Chem. A,* 2013, **1**,112.
[34] W. Xing, C. Liu, Z. Zhou, L. Zhang, J. Zhou, S. Zhuo, Z. Yan, H. Gao, G. Wang, S. Z. Qiao, *Energy Environ. Sci.*, 2012, **5**, 7323.
[35] G. Sethia , A. Sayari, *Carbon*, 2015,**93**, 68.